CANADIAN JOURNAL OF EXPLORATION GEOPHYSICS
VOL. 26, NOS 1 & 2 (DECEMBER 1990), P. 94-103

EFFECTS OF LITHOLOGY, POROSITY AND SHALINESS ON *P*- AND *S*-WAVE VELOCITIES FROM SONIC LOGS

SUSAN L.M. MILLER[1] AND ROBERT R. STEWART[1]

ABSTRACT

Full-waveform sonic logs from four wells in the Medicine River field of Alberta are analyzed for relationships between *P*-wave velocity (V_P), *S*-wave velocity (V_S), V_P/V_S and lithology, shaliness and porosity. V_P/V_S in conjunction with V_P effectively identifies sandstone, limestone and shale lithologies in the sampled intervals. V_P increases quasi-linearly with V_S in sandstone and limestone. Average V_P/V_S values of 1.60 for sandstone and 1.89 for limestone are found. In formations with mixed carbonate/clastic silicate lithologies (the Nordegg, Shunda and Detrital), V_P increases approximately linearly with V_S. The V_P/V_S ratios in the mixed lithologies are bounded by the V_P/V_S values for the component lithologies.

In the sandstones considered here, both V_P and V_S decrease as porosity increases but V_S dependence on porosity is very weak. The V_P/V_S ratio decreases as porosity increases. An increase in shale content lowers V_P and V_S but increases V_P/V_S. Porosity has a greater influence on velocity than shaliness by about an order of magnitude. Both V_P and V_S decrease as porosity increases in the limestone data but the correlation is poor between V_P/V_S and porosity. The linear regression intercepts from the limestone velocity versus porosity plots accurately predict calcite matrix velocities. In the Nordegg, Shunda and Detrital Formations an increase in porosity is accompanied by a decrease in both *P*- and *S*- wave velocities. No V_P/V_S trend is observed in either the Nordegg or the Shunda, but V_P/V_S decreases as porosity increases in the Detrital Formation.

INTRODUCTION

Recording shear waves as well as compressional waves during seismic acquisition and well logging provides additional information about the subsurface (Nations, 1974; Gregory, 1977; Tatham, 1982; Robertson, 1987). Deciphering the lithologic information inherent in seismic elastic-wave velocities requires an understanding of the relationship between geology and velocity. To this end, we are interested in studying the elastic-wave velocity response at the well bore.

Seismic velocities are affected by numerous geologic factors including rock matrix mineralogy, porosity, pore geometry, pore fluid, bulk density, effective stress, depth of burial, type and degree of cementation and degree and orientation of fracturing (McCormack et al., 1985). The complex interaction of these and other factors complicates the task of inverting seismic velocities to obtain petrophysical information. In order to understand how rock properties influence velocity, researchers have employed a variety of approaches such as core analysis, seismic and well log interpretation and numerical modelling (e.g., Kuster and Toksöz, 1974; Gregory, 1977; Eastwood and Castagna, 1983; McCormack et al., 1984).

In the well bore various logging tools provide a number of measurements which describe the subsurface, but in the seismic realm V_P and V_S are the main descriptors available. *S*-wave well logs are crucial in tying observed elastic response to known geology and guiding the interpretation of shear seismic sections. Ultimately, the goal is to invert multicomponent seismic data for petrophysical information.

This paper considers four wells in the Medicine River oil field of central Alberta. The objective of this study is to analyze full-waveform sonic logs in the western Canadian basin and search for trends which provide information on lithology, porosity and pore fluid. The approach has been to examine several of the factors which have been studied by previous workers and determine if trends are present in these field data.

REVIEW

Work that has been done to date suggests that *S*-wave data in conjunction with *P*-wave data can provide information on lithology, porosity, pore geometry and pore fluid, among other things (e.g., Gregory, 1977; Tatham, 1982; Domenico, 1984).

Compressional seismic velocity alone is not a good lithology indicator because of the overlap in V_P for various

Manuscript received by the Editor July 15, 1990; revised manuscript received October 16, 1990.

[1]Department of Geology and Geophysics, The University of Calgary, Calgary, Alberta T2N 1N4

We are grateful to David Byler, Manager of Technical Services of Suncor Inc., for the donation of well log and lithology information for this study. We would also like to acknowledge helpful suggestions from Dr. John Hopkins and Dr. Terry Gordon of the University of Calgary and Douglas Boyd of Halliburton Logging Services. This work was supported by the Consortium for Research in Elastic Wave Exploration Seismology (CREWES) Project at the University of Calgary.

rock types. The additional information provided by shear velocity can reduce the ambiguity involved in interpretation. Pickett (1963) demonstrated the potential of V_P/V_S as a lithology indicator through his laboratory research. Using core measurements, he determined V_P/V_S values of 1.9 for limestone, 1.8 for dolomite, 1.7 for calcareous sandstone and 1.6 for clean sandstone. Subsequent research has generally confirmed these values and has also indicated that V_P/V_S values in mixed lithologies vary linearly between the V_P/V_S ratios of the end members (Nations, 1974; Kithas, 1976; Eastwood and Castagna, 1983; Rafavich et al., 1984; Wilkens, 1984; Castagna et al., 1985).

Various approaches have been taken to analyze the effect of porosity on velocity. These include the time-average equation (Wyllie et al., 1956), the Pickett empirical equation (Pickett, 1963) and the transit-time-to-porosity transform of Raymer et al. (1980). Domenico (1984) used Pickett's data to demonstrate that V_S in sandstones is 2 to 5 times more sensitive to variations in porosity than V_P in sandstones or V_S in limestones. V_P in limestone was found to be the least sensitive porosity indicator.

The model of Kuster and Toksöz indicates that pore-aspect ratio has a strong influence on how V_P and V_S respond to porosity (Kuster and Toksöz, 1974; Toksöz et al., 1976). The actual V_P/V_S ratio appears to be independent of pore geometry unless the aspect ratio is low, less than about 0.01 to 0.05 (Minear, 1982; Tatham, 1982; Eastwood and Castagna, 1983). Modelling suggests that for small-aspect ratio pores such as cracks, V_P/V_S will increase as porosity increases. Robertson (1987) used this model to interpret carbonate porosity from seismic data and correlated an increase in V_P/V_S with an increase in porosity due to elongate pores.

A number of workers have included a clay term in empirical linear regression equations developed from core-analysis data (Tosaya and Nur, 1982; Castagna et al., 1985; Han et al., 1986; King et al., 1988; Eberhart-Phillips et al., 1989). When both porosity and clay effects were studied, porosity was shown to be the dominant effect by a factor of about 3 or 4 (Tosaya and Nur, 1982; Han et al., 1986; King et al., 1988).

Minear (1982) examined the importance of clay on velocities using the Kuster-Toksöz model. Results suggested that dispersed clay has a negligible effect on velocity; however, laminated and structural shale have a similar and significant effect in reducing velocities. Since clay tends to lower the shear modulus of the rock matrix, V_S decreases more than V_P, resulting in an overall increase in V_P/V_S. Tosaya and Nur (1982) concluded that neither clay mineralogy nor location of clay grains were significant factors in the *P*-wave response to clay content.

Because shear velocity is thought to be more sensitive than compressional velocity both to porosity (Domenico, 1984) and to clay content (Minear, 1982), an increase in either component should result in an increase in V_P/V_S. This result has been observed in core studies of clastic silicates (Han et al., 1986; King et al., 1988), seismic surveys over carbonates and sand/shale sequences (McCormack et al., 1984; Anno, 1985; Garotta et al., 1985; Robertson, 1987) and well logging studies of clastic silicates (Castagna et al., 1985). The increase in V_P/V_S with shaliness has been used in seismic field studies to outline sandstone channels encased in shales (McCormack et al., 1984; Garotta et al., 1985).

Eastwood and Castagna (1983) examined full-waveform sonic logs and observed constant V_P/V_S with increasing porosity in an Appalachian limestone and increasing V_P/V_S with increasing porosity in the Frio Formation sandstones and shales.

V_P/V_S is sensitive to gas in most clastics and will often show a marked decrease in its presence (Kithas, 1976; Gregory, 1977; Tatham, 1982; Eastwood and Castagna, 1983; Ensley, 1984, 1985; McCormack et al., 1985). The V_P/V_S response of carbonate rocks to gas is variable, a discrepancy which may be attributable to pore geometry. V_P/V_S reduction has been observed in carbonates with elongate pores (Anno, 1985; Robertson, 1987) and absent in carbonates with rounder pores (Georgi et al., 1989). The gas effect may not be observed on well logs if the depth of penetration does not exceed the invaded zone.

Study Area

The Medicine River field is an oil field in central Alberta (Figure 1) which produces from a number of zones in Cretaceous, Jurassic and Mississippian rocks. The ages and formations of interest are indicated in the stratigraphic chart in Figure 2. The locations of the wells examined in this paper are 9-5-39-3W5, 9-7-39-3W5, 15-18-39-3W5 and 9-13-39-4W5. These are development wells drilled by Suncor Inc. between 1987 and 1989 which are or have been oil producers. The 9-7 and 9-13 wells produce out of the Nordegg Formation, the 15-18 well produces from an interval in the Basal Quartz (Ellerslie) and the 9-5 well produces oil from both the Basal Quartz and the Pekisko Formations. It is difficult to accurately determine the pore-fluid filling in some of the zones as there are no drill stem test data available for any of these wells.

The sandstones sampled in this study are the Basal Quartz sandstone (9-15, 15-18) and the Glauconitic sandstone (all four wells). Watkins (1966) describes the Basal Quartz in this field as a very fine to fine-grained, well-sorted, subangular, quartzitic sandstone. The Glauconitic sandstone is a fine-grained, well-sorted, angular to subangular, quartzose sandstone with siliceous cementation (Watkins, 1966).

The only limestone sampled in this study is from the Pekisko with data from the 9-5 and 15-18 wells. The well site geologist's cuttings log identifies the Pekisko Formation as a slightly dolomitic, slightly argillaceous, crypto to microcrystalline limestone with pinpoint porosity.

The shale points are from the Fernie shale only, with data from the 9-7, 9-13 and 15-18 wells. The Fernie shale is medium to dark grey, platy, fissile, calcareous and micaceous.

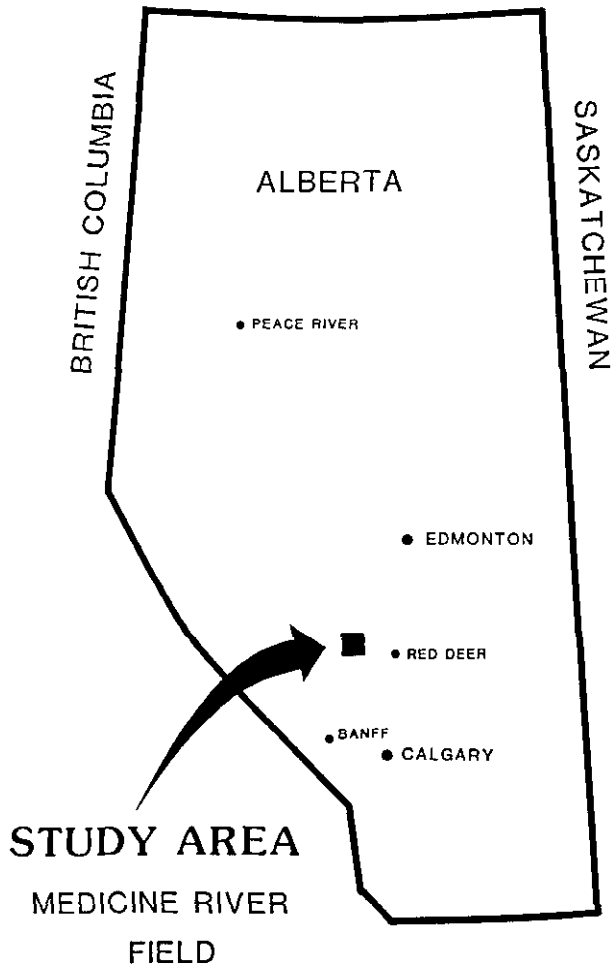

Fig. 1. Location map showing the Medicine River oil field of central Alberta.

Several mixed lithologies were also chosen for analysis. The Nordegg Formation is of Lower Jurassic age and is described by Ter Berg (1966) as a sandstone consisting of medium-sorted, fine-to-medium grained quartz and chert which is cemented by dolomitic limestone. It is sampled in the 9-7 and 9-13 wells, both of which are oil-filled. The Shunda is sampled from the 9-5 well and, according to the well site geologist's cuttings log, consists of interbedded limestone and shale. The core-analysis report describes the Shunda as dolomite with interbedded shale. The Detrital refers to rock detritus on top of the Mississippian unconformity and consists mainly of dolomite in the 9-13 well from which the data is taken.

Based on the available production data and the well logs, the pore fluids present in the Jurassic and Mississippian formations are oil and water.

Methods

The availability of *S*-wave data from these well logs was limited by several factors. The full-waveform sonic logs analyzed in this study were only run over several hundred metres through the zones of interest. Readings from the tool may be suspect in regions of borehole washout. The *S*-wave curve cannot be used in formations in which the *S*-wave velocity is slower than the *P*-wave velocity of the mud as there will be no *S*-wave refraction. In these wells, this occurs in some shales and in all coals and is indicated by warning flags on the log and either off-scale or straight-line *S*-wave transit times.

Those portions of the log where the elastic transit times were judged to be reliable were examined for zones which either represent a particular lithology or are of exploration interest. Intervals were chosen which could be clearly identified using well log curves (e.g., gamma-ray curve) and geological information (e.g., well site geologist's cuttings report). Only intervals which were a minimum of five metres thick were selected for sampling. Data points were not taken from the top and base of the formations where the well log curves were deflecting rapidly.

The well log curves were digitized with readings recorded every metre. Transit times were used to calculate V_p, V_s and V_p/V_s. V_p and V_s are directly used in seismic processing and conventional rock characterization; thus, we prefer to use V_p/V_s instead of introducing the related Poisson's ratio.

The gamma-ray curve was used to compute the gamma-ray index (G) as follows:

$$G = \frac{GR_{log}-GR_{sand}}{GR_{shale}-GR_{sand}}, \quad (1)$$

where GR is the gamma-ray response in GAPI units and GR_{sand} and GR_{shale} values are based on the interpreted sand and shale lines. Various curves are available which can be used to convert the gamma-ray index to clay content, each of which will give significantly different estimates (Heslop, 1974). Heslop observed a linear correlation between gamma-ray response and clay volume as determined by x-ray-diffraction data from core samples. Kukal and Hill (1986) confirmed the linear relationship and noted that most shales contain about 60 percent clay. Based on their analysis, clay volume could be calculated from the expression above by multiplying G by 0.60. Since we do not have available the relationship between shale and clay content for this area, we have chosen to use a simple linear relationship between gamma-ray deflection and shale content. In this study we have used the gamma-ray index (x 100) as a measure of percentage shaliness.

Porosities were calculated using neutron-density crossplots and, when the data were available, bulk density and photoelectric absorption crossplots. Porosity values were corrected for shale content in the sandstone data. Gamma-ray readings are most likely due to shale content in these formations (J. Hopkins, 1990, pers. comm.) and were therefore used as a measure of shale volume. Neutron porosity and density porosity values from surrounding shales were used to determine the shale point on the crossplot. This point was used to create a scale from 0 to 100 percent shale so that the required correction for a given percentage of shale could be determined. The neutron-

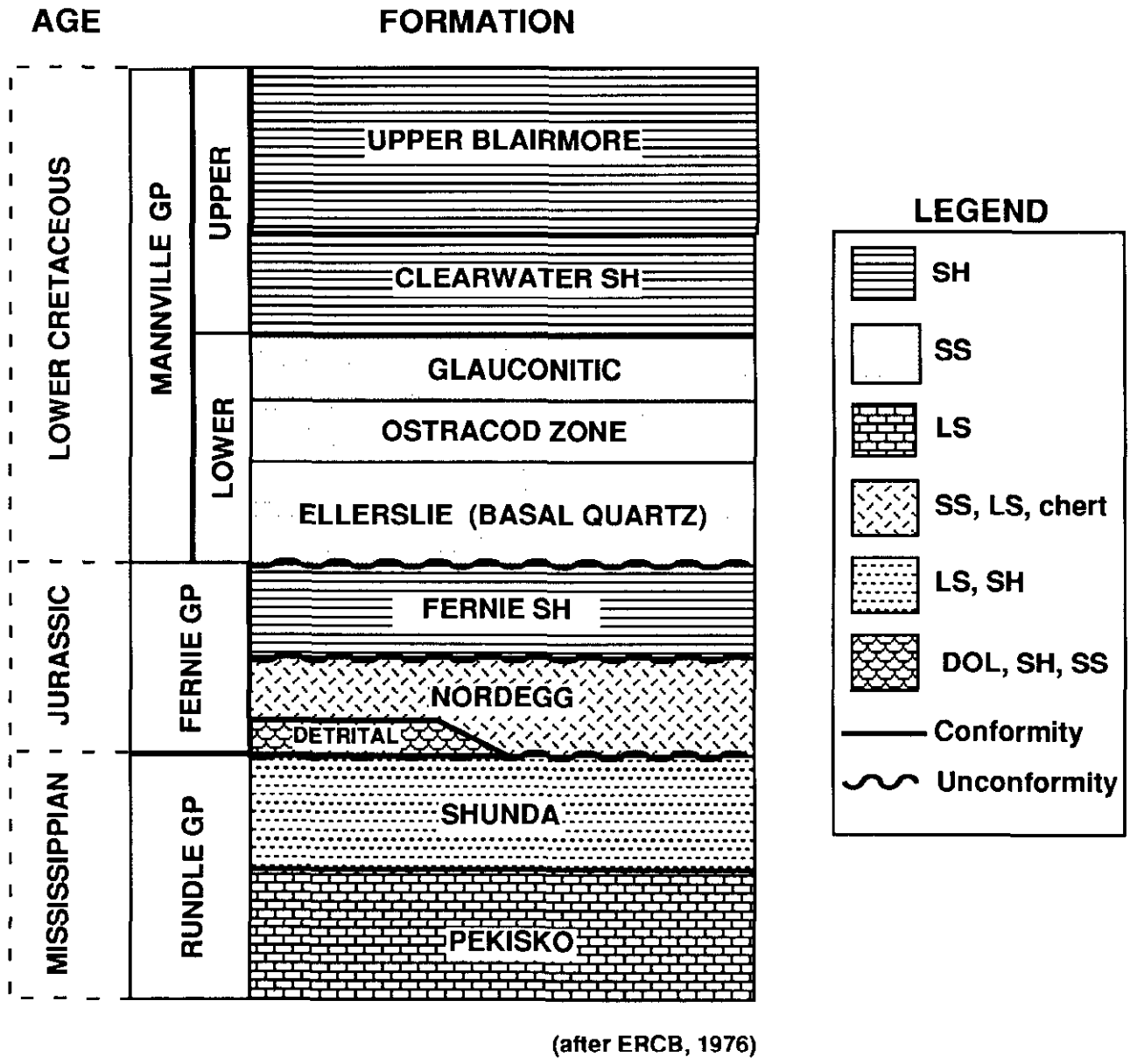

Fig. 2. Stratigraphic chart of the ages and formations of interest. The lithologies studied are shale (SH), sandstone (SS), limestone (LS), dolomite (DOL) and complex mixtures of these.

density porosity values were then shifted toward the clean lithology lines by the corresponding correction factor.

Porosity values from the Nordegg and Detrital Formations were not corrected for shaliness as the radioactivity in these units may be due to rock fragments rather than shale (J. Hopkins, 1990, pers. comm.). The uncorrected crossplot porosities agreed with other porosity measurements as described below. Although the Shunda has shale interbeds, uncorrected crossplot porosity values tracked core measurements in the vicinity closely.

Neutron-density crossplot porosity values were compared to porosity data from two other sources to check their reliability. The values for all formations are the same as or close (within 1 or 2 porosity percentage units) to those determined by a computer-processed interpretation which incorporates a suite of environmentally corrected log curves. Core reports from the 9-5 and 15-18 wells were examined although core porosity values were not available for the exact depths studied in this analysis. Neutron-density crossplot porosities from nearby units were generally within 1 or 2 porosity percentage units of available core porosities. At two depths the FDC values were closer to the core porosity than the crossplot values, but overall the crossplot corresponded most closely to core measurements. Porosity

values were not taken in shales due to the difficulty of obtaining meaningful values.

The effect of pressure on velocity has been examined in laboratory work (Pickett, 1963; Gregory, 1977; Domenico, 1984; Han et al., 1986; King, 1988; Eberhart-Phillips et al., 1989). Velocities generally increase rapidly initially but stabilize at higher pressures. The formations examined in this paper are all at depths between 2000 and 2200 metres, giving an effective stress of about 25 MPa (3600 psi). At this depth, pressure effects have levelled off and should be similar for all the formations.

Analysis involved crossplotting of velocity, slowness, velocity ratio, porosity and percentage shale for the selected units in each of the four wells. These plots were examined for trends. We have used single and multivariate linear regression analysis to assess the relationship between the various parameters. In regression analysis the independent variable is assumed to be error-free. This is not the case for porosity or shale data obtained from well logs; however, the analysis is conventionally held to be a valid means of studying velocity dependence on these variables (Troutman and Williams, 1987).

Well cuttings log depths sometimes differed from wireline log depths and required adjustment using a suitable geologic marker, such as coal, for reference. All depths referred to in this paper are sonic-log depths.

Results

Lithology effects

Figure 3 is a plot of V_p vs V_s for sandstone, limestone and shale for all four wells. The superimposed lines have slopes of 1.9 and 1.6, the conventional V_p/V_s ratios for limestone and sandstone, respectively. The sandstone data points are scattered around the V_p/V_s value of 1.6 and have an average V_p/V_s ratio of 1.60. The limestone data have an average V_p/V_s ratio of 1.89. Within the range of data represented here, V_p appears to be approximately linearly related to V_s for both sandstone and limestone. Correlation coefficients (r) are 0.88 and 0.89, respectively. The V_p/V_s values for both lithologies and the good correlations between V_p and V_s are consistent with the observations of other investigators. Shale does not show a strong linear correlation between V_p and V_s ($r = 0.29$) but has an average V_p/V_s ratio of 1.89. V_p/V_s is quite variable for shales; however, the average value observed here falls within the range used by Minear (1982) and is comparable to the value of 1.936 used by Eastwood and Castagna (1983) for modelling.

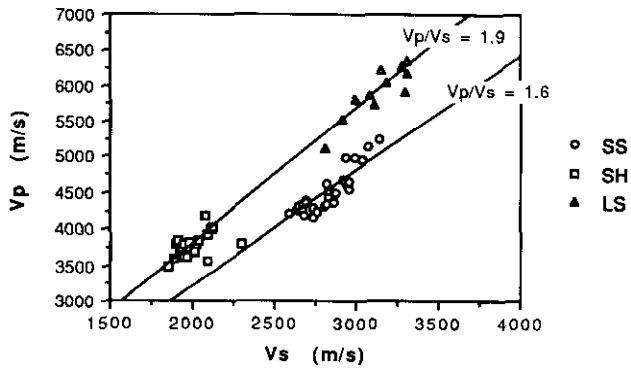

Fig. 3. V_p vs V_s for sandstone (SS), limestone (LS) and shale (SH) lithologies. The data are from full-waveform sonic logs from the Medicine River field. Lines of constant V_p/V_s are superimposed on the data points.

The data have been replotted in Figure 4 to demonstrate the effectiveness of using V_p/V_s and V_p to differentiate the pure lithologies in this data set. Although the V_p values for sandstone and shale compressional velocities overlap at about 4200 m/s and sandstone and limestone overlap at about 5200 m/s, the lithology types are differentiated by the addition of V_p/V_s values.

Several complex lithologies are also examined. The Nordegg, Shunda and Detrital are mixtures of carbonates and clastics and plot between the sandstone and limestone end members with average V_p/V_s values of 1.75, 1.76 and 1.76, respectively (Figure 5). Clearly, complex lithologies can cause ambiguities in the interpretation of velocity data. The mixed lithologies of the Nordegg, Detrital and Shunda show approximately linear relationships between V_p and V_s with correlation coefficients of 0.84, 0.91, and 0.92, respectively (Figure 6).

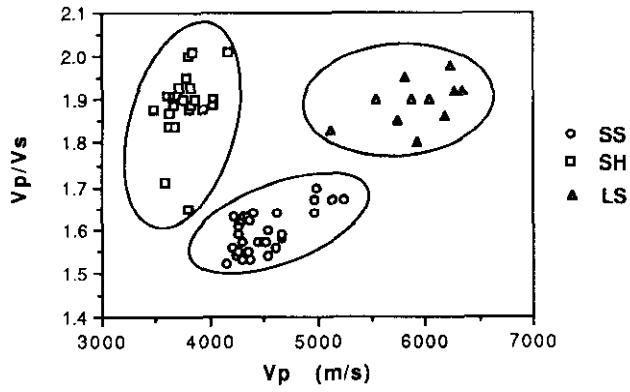

Fig. 4. V_p/V_s vs V_p for sandstone, limestone and shale. The data from Figure 3 are replotted to demonstrate the separation of lithologies.

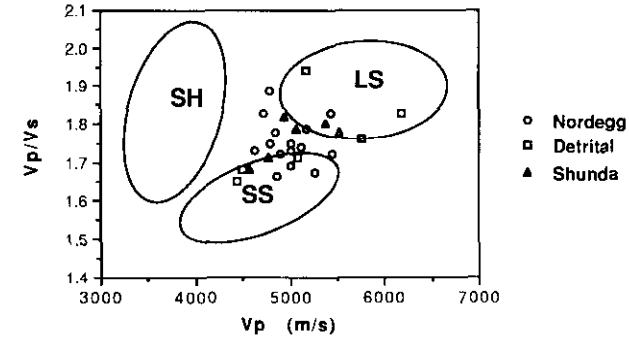

Fig. 5. V_p/V_s vs V_p for complex lithologies. The Nordegg, Shunda and Detrital are formations with mixed carbonate/clastic silicate lithologies. The superimposed outlines from Figure 4 show that the V_p/V_s ratios for mixed rock types plot between the ratios of the component lithologies.

The functional relationship between V_P and V_S for different rock types is still open to question. We have considered the V_P/V_S ratio, which is an average value, and the linear correlation between V_P and V_S. The significance of the slope and intercept values obtained from regression analysis and how they relate to physical rock properties is a subject for further investigation. Ikwuakor (1988) suggests that the slopes and intercept values derived from linear velocity relationships are better indicators of lithology than V_P/V_S and may also contain other geologic information. However, for small data sets with inherent uncertainty in the measurements, accurate and repeatable slope and intercept values may be difficult to obtain.

Porosity and shale effects

The highest correlation coefficients for these data are obtained when velocity (rather than slowness or traveltime difference) is plotted against porosity. Results for the sandstone data are shown in Figure 7. *P*-wave velocity shows a weak dependence on porosity. The extracted V_P intercept value indicates a sandstone matrix velocity of 5028 m/s – somewhat lower than the range of 5486 to 5944 m/s given by Gregory (1977). An unexpected observation is in the *S*-wave velocity, which shows a very weak dependence on porosity. This differs from the previous studies cited which found *S*-wave velocities in sandstones to be highly sensitive to variations in porosity. Residual analysis on both data sets suggests that there may be a higher order dependence. However, the number of data points is too limited to warrant extensive statistical manipulation. The greater sensitivity of V_P results in an overall decrease in V_P/V_S (Figure 8), a result which also differs from research previously cited. The large scatter and relatively low correlation coefficient of 0.65 indicate caution in interpreting these results.

In an attempt to improve the fit to the data we have used multivariate linear regression with porosity and shale fraction as independent variables. The data suggests that porosity is weakly dependent on shale content, so that the results should again be viewed with caution. Addition of a shale term improves the correlation somewhat and also increases the intercepts, or predicted sandstone matrix velocities. The best fit was obtained by plotting velocity, rather than slowness, as the dependent variable. Multivariate linear regression with linear terms produced the following relationships:

$$V_P \text{ (km/s)} = 5.30 - 7.12\varnothing - 0.44\kappa \qquad r = 0.51, \qquad (2)$$

$$V_S \text{ (km/s)} = 3.16 - 2.62\varnothing - 0.38\kappa \qquad r = 0.32, \text{ and} \qquad (3)$$

$$V_P/V_S = 1.68 - 0.99\varnothing + 0.056\kappa \qquad r = 0.66, \qquad (4)$$

where $\varnothing$ = fractional porosity,
κ = fractional shale, and
r = correlation coefficient.

These relationships are calculated over a porosity range of 0.04 to 0.14 and a shale range from 0.01 to 0.44. The standard error is about 5 percent for V_P and V_S and 2 percent for V_P/V_S. The standard error of the porosity coefficients is almost 40 percent in the expressions for V_P and V_P/V_S and 56 percent in the equation for V_S. The large uncertainty in the coefficients suggests that these expressions are more useful for describing trends in the data rather than predicting values. The standard error in the shale coefficient is sometimes as high as the coefficient itself. However, the magnitude of the coefficient is small, so that the effect on predicted velocities is also small.

The intercepts in equations (2) and (3) are similar to those obtained by Tosaya and Nur (1982), Castagna et al. (1985), Han et al. (1986) and Eberhart-Phillips et al. (1989). The coefficient for the porosity term in equation (2) is also similar in magnitude to those quoted by these workers, but the porosity coefficient in equation (3) is 40 to 60 percent lower, emphasizing again the lack of V_S sensitivity to porosity in these data. We see this effect in equation (4), which shows that V_P/V_S will increase as porosity decreases.

These equations also differ from those of the investigators referred to above in that the shale coefficient is lower than the porosity coefficient by about an order of magnitude rather than by a factor of 3 or 4. Although porosity is somewhat dependent on shale content in these data, plots of velocity and shale content indicate a minor effect from shale. If we use clay fraction rather than shale fraction (where shale is assumed to be composed of 60 percent clay), the coefficient for κ increases by about 67 percent in each of these equations.

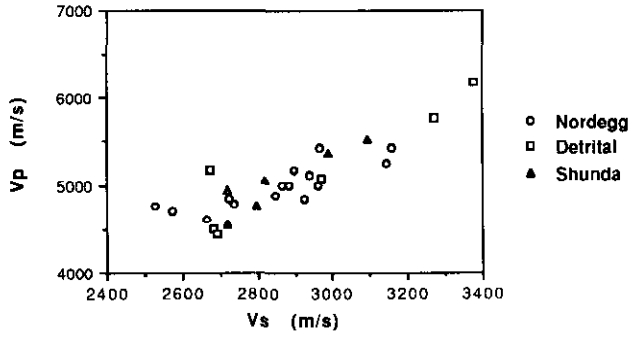

Fig. 6. V_P vs V_S for complex lithologies. Approximately linear relationships exist between V_P and V_S for the Nordegg, Shunda and Detrital Formations.

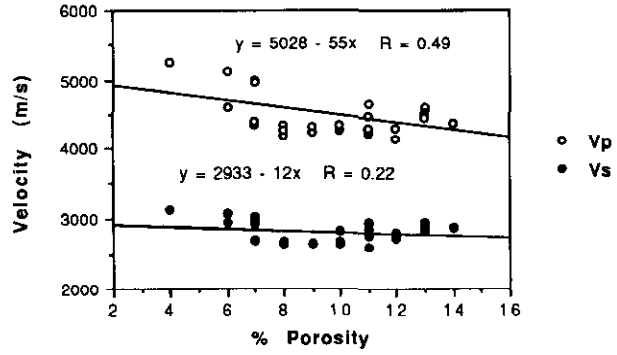

Fig. 7. V_P and V_S vs percent porosity for sandstone. Data are from the Glauconitic and Basal Quartz sandstones. V_P shows a weak dependence on porosity in sandstone, decreasing by 15 to 20% as porosity increases from 4 to 14%. V_S is fairly insensitive to porosity variations.

The relative magnitudes of the shale coefficients indicate that V_S is more sensitive to the addition of shale than V_P. This results in an apparent increase in V_P/V_S with increasing shaliness (Figure 9). This trend is consistent with the observations of the other researchers cited.

Eberhart-Phillips et al. (1989) found that using the square root of clay content improved the fit as it accounted for the large change in velocity observed when only a small amount of clay was present. Use of the square root term here improved the correlation marginally; however, the data contain too much scatter to support a more complex term.

The data were also analyzed for the response of a particular formation from well to well. Variations in V_P/V_S response within the same formation should be attributable to changes in porosity, pore fluid or facies. The Basal Quartz sandstone is sampled from the 9-5 well (2144 to 2148 m) and the 15-18 well (2170 to 2174 m). The portion of the Basal Quartz sampled in the 9-5 well averages about 13 percent porosity, 4 percent shale and is oil-saturated. In the 15-18 well, the Lower Basal Quartz section which is sampled averages about 6 percent porosity, 35 percent shale and is water-saturated. The data points from the two wells separate distinctly on a crossplot of V_P/V_S vs V_P (Figure 10). The sampled interval from the relatively clean, porous, oil-saturated 9-5 well has both a lower P-wave velocity and a lower V_P/V_S ratio than the shalier, tighter, water-saturated interval in the 15-18 well. This separation could be due to a difference in porosity, shale, pore fluid, or some combination thereof. The production GOR (gas/oil ratio) for the 9-5 well is about 150 which is quite high for this formation. This suggests that gas might be a factor in reducing V_P and, thus, V_P/V_S in this well.

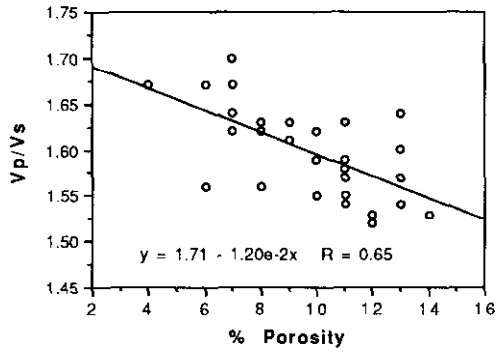

Fig. 8. V_P/V_S vs percent porosity for sandstone. The data are scattered but the velocity ratio shows an apparent tendency to decrease as porosity increases in sandstone.

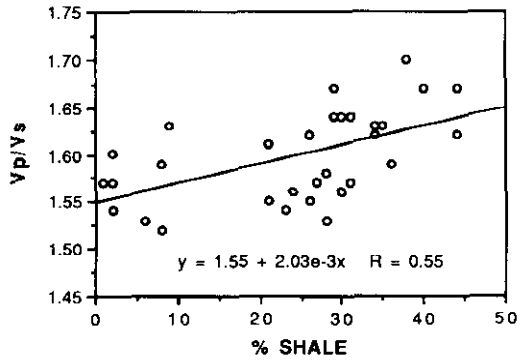

Fig. 9. V_P/V_S vs percent shale for sandstone. V_P/V_S may exhibit a slight trend of increasing V_P/V_S as the shale content of the sandstone increases.

Plots of velocity vs porosity for the Pekisko limestone indicate that both V_P and V_S are dependent on porosity (Figure 11). The intercepts represent limestone matrix velocities and are very close to the V_P (6259 m/s) and V_S (3243 m/s) values for calcite quoted by Domenico (1984). The V_P/V_S ratio for the limestone matrix is about 1.9 as predicted but shows little change as porosity increases (Figure 12). This is consistent with findings by Eastwood and Castagna (1983). It is also the response predicted by Kuster-Toksöz modelling in a saturated limestone in which the majority of pores are round, i.e., have high-aspect ratios (Robertson, 1987). This is likely to be the case with the Pekisko which has pinpoint porosity (secondary porosity with voids <1/16 mm).

Velocity and porosity data from the Nordegg, Shunda and Detrital Formations are plotted in Figures 13 through 15, respectively. In each case, both V_P and V_S show a dependence on porosity. Both V_P and V_S show a similar decrease as porosity increases in the Nordegg Formation. In the case of the Shunda, V_P appears to be slightly more sensitive than V_S to the rise in porosity, but the porosity range is very limited. In the Detrital Formation, P-wave velocity decreases more rapidly than S-wave velocity for an overall decrease in V_P/V_S. This decrease is consistent with the observations for the sandstones but differs from the previously cited results by a number of other researchers.

Conclusions

Data obtained from full-waveform sonic logs indicate that V_P with V_S successfully discriminate between sandstone, limestone and shale lithologies. Average V_P/V_S ratios

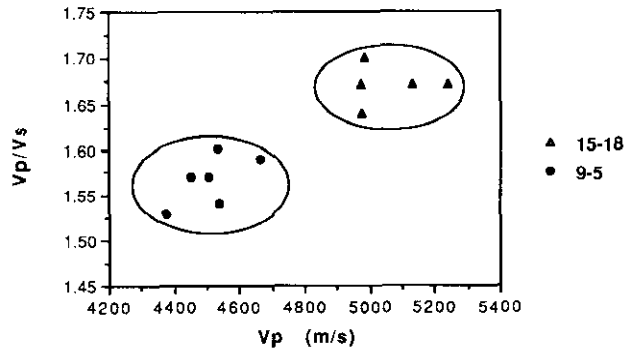

Fig. 10. V_P/V_S vs V_P for the Basal Quartz sandstone. The data points from the 9-5 well, which averages about 13% porosity, 4% shale and is oil-saturated, are separated from the 15-18 well which averages about 6% porosity, 35% shale and is water-saturated.

are 1.60 for sandstones and 1.89 for limestone and shale. Complex lithologies have V_p/V_s ratios which plot between the values of their component rock types. This may cause ambiguities in interpretation. V_p is approximately linearly correlated with V_s in the lithologies studied here.

Seismic velocities in sandstone are affected by variations in porosity and shaliness, with porosity having a stronger effect. Multivariate linear regression results in three relationships which describe the trends observed in the data. These relationships indicate that V_p decreases as porosity increases. V_s in these sandstones is relatively insensitive to changes in porosity, showing only a slight reduction. As a result, the V_p/V_s ratio decreases with increasing porosity. This observation differs from that quoted by several other investigators, who observed an increase in V_p/V_s with rising porosity.

Porosity has a greater influence on velocity than shaliness by about an order of magnitude, but our correlations suggest that an increase in shale content will lower V_p and V_s and cause the V_p/V_s ratio to rise. The increase in V_p/V_s agrees with observations by other workers; however, in these data the effect of the shale is substantially smaller.

Data from the Pekisko limestone indicate that both V_p and V_s decrease as porosity increases but the V_p/V_s ratio exhibits little trend with rising porosity. This is the response predicted by Kuster-Toksöz modelling for limestones in which the pores tend to be round, which is probably the case for the pinpoint porosity of the Pekisko. The linear regression intercepts from the limestone velocity-vs-porosity plots accurately predict calcite matrix velocities.

P-wave and *S*-wave velocities decrease as porosity increases in the carbonate/clastic lithologies of the Nordegg, Shunda and Detrital Formations. V_p/V_s decreases as porosity increases in the Detrital but does not demonstrate a porosity trend in either the Nordegg or the Shunda.

A number of trends were visible in these field data, suggesting that *P*- and *S*-wave data can contribute valuable information about the subsurface. In particular, velocities contain information on lithology, porosity and the degree of shaliness.

References

Anno, P.D., 1985, Exploration of the Hunton Group, Anadarko Basin, using shear waves: Presented at the 53rd Ann. Internat. Mtg., Soc. Expl. Geophys., Las Vegas.

Castagna, J.P., Batzle, M.L. and Eastwood, R.L., 1985, Relationships between compressional-wave and shear-wave velocities in clastic silicate rocks: Geophysics **50**, 571-581.

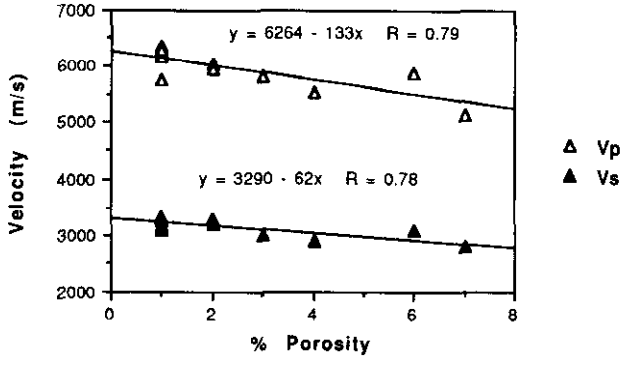

Fig. 11. V_p and V_s vs percent porosity for the Pekisko limestone. V_p and V_s both appear to be dependent on porosity variations: y-intercepts represent limestone matrix velocities.

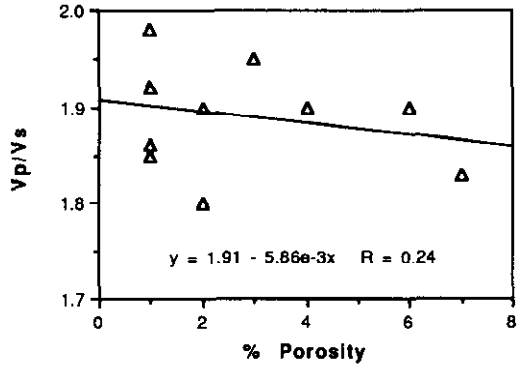

Fig. 12. V_p/V_s vs percent porosity for the Pekisko limestone. Both V_p and V_s show a similar response to porosity variation so there is little overall trend for the V_p/V_s ratio.

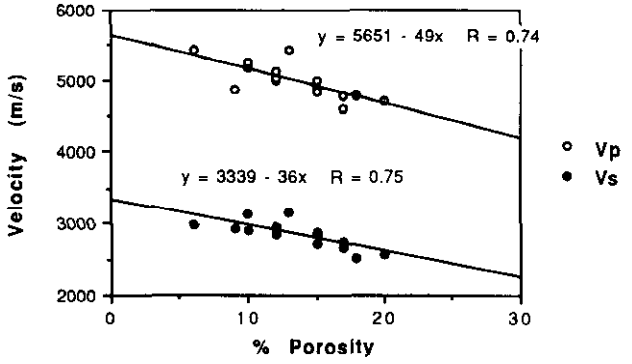

Fig. 13. V_p and V_s vs percent porosity for the Nordegg Formation. The Nordegg is a mixture of sandstone, limestone and chert and is one of the oil-producing zones in the Medicine River field. Both V_p and V_s show a similar degree of dependence on porosity.

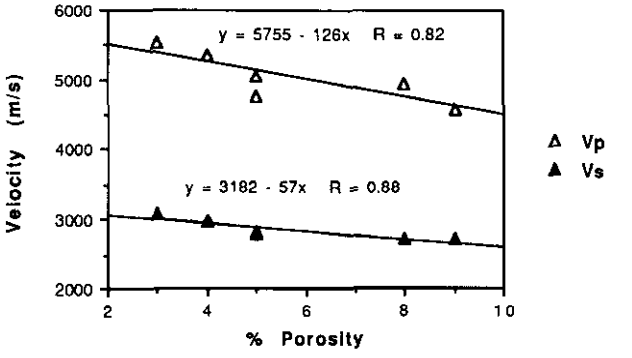

Fig. 14. V_p and V_s vs percent porosity for the Shunda Formation. The Shunda is a Mississippian carbonate with shale stringers. The range of variation of porosity is very limited, but both V_p and V_s show a linear decrease as porosity increases with V_p responding slightly more than V_s.

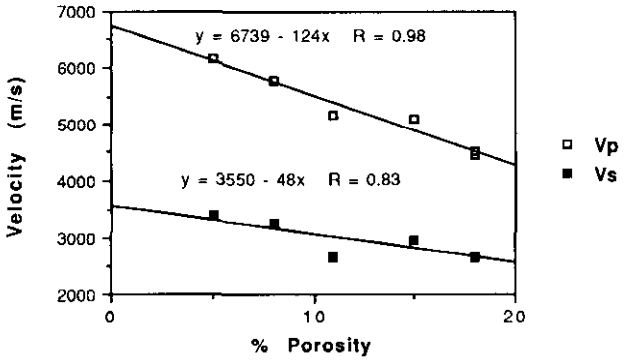

Fig. 15. V_P and V_S vs percent porosity for the Detrital. The Detrital refers to rock detritus on top of the Mississippian unconformity. It is composed largely of dolomite in the well from which the data points are taken. The velocity data exhibit a dependence on porosity; the more rapid decline of V_P results in a decrease in the V_P/V_S ratio.

Eastwood, R.L. and Castagna, J.P., 1983, Basis for interpretation of V_P/V_S ratios in complex lithologies: 24th Ann. Logging Symp., Soc. Prof. Well Log Analysts, Calgary.

Eberhart-Phillips, D., Han, D.H. and Zoback, M.D., 1989, Empirical relationships among seismic velocity, effective pressure, porosity, and clay content in sandstone: Geophysics **54**, 82-89.

Ensley, R.A., 1984, Comparison of *P*- and *S*-wave seismic data: a new method for detecting gas reservoirs: Geophysics **49**, 1420-1431.

_____, 1985, Evaluation of direct hydrocarbon indicators through comparison of compressional- and shear-wave seismic data: a case study of the Myrnam gas field, Alberta: Geophysics **50**, 37-48.

Garotta, R., Marechal, P. and Megesan, M., 1985, Two-component acquisition as a routine procedure for recording *P*-waves and converted waves: J. Can. Soc. Expl. Geophys. **21**, 40-53.

Georgi, D.T., Heavysege, R.G., Chen, S.T. and Eriksen, E.A., 1989, Application of shear and compressional transit-time data to cased hole carbonate reservoir evaluation: 12th Formation Evaluation Symp., Can. Well Logging Soc., Calgary.

Gregory, A.R., 1977, Aspects of rock physics from laboratory and log data that are important to seismic interpretation, *in* Seismic Stratigraphy — applications to hydrocarbon exploration: Am. Assn. Petr. Geol., Mem. 26, 15-45.

Han, D.H., Nur, A. and Morgan, D., 1986, Effects of porosity and clay content on wave velocities in sandstones: Geophysics **51**, 2093-2107.

Heslop, A., 1974, Gamma-ray log response of shaly sandstones: 15th Ann. Symp., Soc. Prof. Well Log Analysts, McAllen, Texas.

Ikwuakor, K.C., 1988, V_P/V_S revisited: pitfalls and new interpretation techniques: World Oil **207**, 3, 41-46.

King, M.S., Stauffer, M.R., Yang, H.J.P. and Hajnal, Z., 1988, Elastic-wave and related properties of clastic rocks from the Athabasca basin, western Canada: Can. J. Expl. Geophys., **24**, 110-116.

Kithas, B.A., 1976, Lithology, gas detection, and rock properties from acoustic logging systems: 17th Ann. Symp., Soc. Prof. Well Log Analysts, Denver.

Kukal, G.C. and Hill, R.E., 1986, Log analysis of clay volume: an evaluation of techniques and assumptions used in an Upper Cretaceous sand-shale sequence: 27th Ann. Symp., Soc. Prof. Well Log Analysts, Houston.

Kuster, G.T. and Toksöz, M.N., 1974, Velocity and attenuation of seismic waves in two-phase media: Part 1, Theoretical formulations: Geophysics **39**, 587-606.

McCormack, M.D., Dunbar, J.A. and Sharp, W.W., 1984, A case study of stratigraphic interpretation using shear and compressional seismic data: Geophysics **49**, 509-520.

_____, _____ and _____, 1985, A stratigraphic interpretation of shear and compressional wave seismic data for the Pennsylvanian Morrow formation of southeastern New Mexico, *in* Seismic Stratigraphy II: Am. Assn. Petr. Geol., Mem. 39, 225-239.

Minear, J.W., 1982, Clay models and acoustic velocities: 57th Ann. Tech. Conf. and Exhib., Soc. Petr. Eng. of AIME, New Orleans.

Nations, J.F., 1974, Lithology and porosity from acoustic shear and compressional wave transit time relationships: 15th Ann. Symp., Soc. Prof. Well Log Analysts, McAllen, Texas.

Pickett, G.R., 1963, Acoustic character logs and their applications in formation evaluation: J. Can. Petr. Tech. **15**, 659 - 667.

Rafavich, F., Kendall, C.H.St.C. and Todd, T.P., 1984, The relationship between acoustic properties and the petrographic character of carbonate rocks: Geophysics **49**, 1622 - 1636.

Raymer, L.L., Hunt, E.R. and Gardner, J.S., 1980, An improved sonic transit time-to-porosity transform: 21st Ann. Symp., Soc. Prof. Well Log Analysts, Lafayette.

Robertson, J.D., 1987, Carbonate porosity from S/P traveltime ratios: Geophysics **52**, 1346-1354.

Tatham, R.T., 1982, V_P/V_S and lithology: Geophysics **47**, 336-344.

Ter Berg, L.J.A., 1966, Medicine River field, *in* Century, J.R., Ed., Oil fields of Alberta supplement: Alberta Society of Petroleum Geologists, 70-71.

Toksöz, M.N., Cheng, C.H. and Timur, A., 1976, Velocities of seismic waves in porous rocks: Geophysics **41**, 621-645.

Tosaya, C. and Nur, A., 1982, Effects of diagenesis and clays on compressional velocities in rocks: Geophys. Res. Lett. **9**, 5-8.

Troutman, B.M. and Williams, G.P., 1987, Fitting straight lines in the earth sciences, *in* Size, W.B., Ed., Use and abuse of statistical methods in the earth sciences: Studies in mathematical geology No. 1, Oxford Univ. Press, inc. 107-128.

Watkins, P.B., 1966, Medicine River oil field, *in* Century, J.R., Ed., Oil fields of Alberta supplement: Alberta Society of Petroleum Geologists, 62-65.

Wilkens, R., Simmons, G. and Caruso, L., 1984, The ratio V_P/V_S as a discriminant of composition for siliceous limestones: Geophysics **49**, 1850-1860.

Wyllie, M.R.J., Gregory, A.R. and Gardner, L.W., 1956, Elastic wave velocities in heterogeneous and porous media: Geophysics **21**, 41-70

APPENDIX

	Lithology	Formation	Well Location	Depth (m)	V_P (m/s)	V_S (m/s)	V_P/V_S	% Shale	% Porosity
1								(G x 100)	
2	Sandstone	Glauconitic	9-5-39-3W5	2100	4152	2734	1.52	8	12
3	Sandstone	Glauconitic	9-5-39-3W5	2101	4220	2588	1.63	9	11
4	Sandstone	Glauconitic	9-5-39-3W5	2102	4600	2947	1.56	24	6
5	Sandstone	Glauconitic	9-5-39-3W5	2103	4403	2692	1.64	30	7
6	Sandstone	Glauconitic	9-7-39-3W5	2117	4305	2808	1.53	28	12
7	Sandstone	Glauconitic	9-7-39-3W5	2118	4619	2816	1.64	31	13
8	Sandstone	Glauconitic	9-7-39-3W5	2119	4490	2858	1.57	27	11
9	Sandstone	Glauconitic	9-7-39-3W5	2120	4659	2953	1.58	28	11
10	Sandstone	Glauconitic	9-7-39-3W5	2121	4294	2744	1.57	31	11
11	Sandstone	Glauconitic	15-18-39-3W5	2116	4234	2758	1.54	23	11
12	Sandstone	Glauconitic	15-18-39-3W5	2117	4266	2675	1.59	36	10
13	Sandstone	Glauconitic	15-18-39-3W5	2118	4198	2682	1.56	30	8
14	Sandstone	Glauconitic	15-18-39-3W5	2119	4319	2651	1.63	35	9
15	Sandstone	Glauconitic	15-18-39-3W5	2120	4353	2814	1.55	26	10
16	Sandstone	Glauconitic	15-18-39-3W5	2121	4273	2645	1.62	44	8
17	Sandstone	Glauconitic	9-13-39-4W5	2147	4348	2673	1.63	34	8
18	Sandstone	Glauconitic	9-13-39-4W5	2148	4361	2695	1.62	34	7
19	Sandstone	Glauconitic	9-13-39-4W5	2149	4302	2648	1.62	26	10
20	Sandstone	Glauconitic	9-13-39-4W5	2150	4260	2744	1.55	21	11
21	Sandstone	Glauconitic	9-13-39-4W5	2151	4253	2638	1.61	21	9
22	Sandstone	Basal Quartz	9-5-39-3W5	2144	4375	2866	1.53	6	14
23	Sandstone	Basal Quartz	9-5-39-3W5	2145	4508	2872	1.57	1	13
24	Sandstone	Basal Quartz	9-5-39-3W5	2146	4449	2830	1.57	2	13
25	Sandstone	Basal Quartz	9-5-39-3W5	2147	4540	2955	1.54	2	13
26	Sandstone	Basal Quartz	9-5-39-3W5	2148	4534	2835	1.60	2	13
27	Sandstone	Basal Quartz	9-5-39-3W5	2149	4666	2925	1.59	8	11
28	Sandstone	Basal Quartz	15-18-39-3W5	2170	4975	2984	1.67	29	7
29	Sandstone	Basal Quartz	15-18-39-3W5	2171	4973	3035	1.64	29	7
30	Sandstone	Basal Quartz	15-18-39-3W5	2172	4985	2927	1.70	38	7
31	Sandstone	Basal Quartz	15-18-39-3W5	2173	5132	3073	1.67	40	6
32	Sandstone	Basal Quartz	15-18-39-3W5	2174	5240	3139	1.67	44	4
33	Limestone	Pekisko	9-5-39-3W5	2183	5732	3103	1.85	15	7
34	Limestone	Pekisko	9-5-39-3W5	2184	6278	3271	1.92	8	1
35	Limestone	Pekisko	9-5-39-3W5	2185	6171	3311	1.86	5	2
36	Limestone	Pekisko	9-5-39-3W5	2186	6347	3302	1.92	3	4
37	Limestone	Pekisko	9-5-39-3W5	2187	5927	3293	1.80	10	3
38	Limestone	Pekisko	9-5-39-3W5	2188	5867	3081	1.90	4	1
39	Limestone	Pekisko	15-18-39-3W5	2193	5127	2803	1.83	15	1
40	Limestone	Pekisko	15-18-39-3W5	2194	6226	3151	1.98	10	1
41	Limestone	Pekisko	15-18-39-3W5	2195	6037	3183	1.90	1	1
42	Limestone	Pekisko	15-18-39-3W5	2196	5531	2910	1.90	20	2
43	Limestone	Pekisko	15-18-39-3W5	2197	5814	2987	1.95	20	6
44	Shale	Fernie	9-7-39-3W5	2167	4175	2080	2.01	–	–
45	Shale	Fernie	9-7-39-3W5	2168	3841	1910	2.01	–	–
46	Shale	Fernie	9-7-39-3W5	2169	3653	1935	1.89	–	–
47	Shale	Fernie	9-7-39-3W5	2170	3855	2030	1.90	–	–
48	Shale	Fernie	9-7-39-3W5	2171	3789	1944	1.95	–	–
49	Shale	Fernie	9-7-39-3W5	2172	3624	1940	1.87	–	–
50	Shale	Fernie	9-7-39-3W5	2173	3926	2086	1.88	–	–
51	Shale	Fernie	9-7-39-3W5	2174	3662	1920	1.91	–	–
52	Shale	Fernie	9-7-39-3W5	2175	3578	2092	1.71	–	–
53	Shale	Fernie	15-18-39-3W5	2177	3798	1895	2.00	–	–
54	Shale	Fernie	15-18-39-3W5	2178	3684	2006	1.84	–	–
55	Shale	Fernie	15-18-39-3W5	2179	3796	2295	1.65	–	–
56	Shale	Fernie	15-18-39-3W5	2180	3478	1849	1.88	–	–
57	Shale	Fernie	15-18-39-3W5	2181	3646	2129	1.71	–	–
58	Shale	Fernie	9-13-39-4W5	2180	3821	1980	1.93	–	–
59	Shale	Fernie	9-13-39-4W5	2181	4021	2126	1.89	–	–
60	Shale	Fernie	9-13-39-4W5	2182	4018	2117	1.90	–	–
61	Shale	Fernie	9-13-39-4W5	2183	3812	2027	1.88	–	–
62	Shale	Fernie	9-13-39-4W5	2184	3752	1976	1.90	–	–
63	Shale	Fernie	9-13-39-4W5	2185	3714	1920	1.93	–	–
64	Shale	Fernie	9-13-39-4W5	2186	3830	2025	1.89	–	–
65	Shale	Fernie	9-13-39-4W5	2187	3689	1927	1.91	–	–
66	Shale	Fernie	9-13-39-4W5	2188	3601	1890	1.91	–	–
67	Shale	Fernie	9-13-39-4W5	2189	3625	1970	1.84	–	–
68	SS, LS, chert	Nordegg	9-7-39-3W5	2176	5435	2968	1.83	(14)	6
69	SS, LS, chert	Nordegg	9-7-39-3W5	2177	5262	3144	1.67	(24)	10
70	SS, LS, chert	Nordegg	9-7-39-3W5	2178	5001	2886	1.73	(22)	15
71	SS, LS, chert	Nordegg	9-7-39-3W5	2179	4794	2737	1.75	(31)	17
72	SS, LS, chert	Nordegg	9-7-39-3W5	2180	4782	2529	1.89	(41)	18
73	SS, LS, chert	Nordegg	9-7-39-3W5	2181	4715	2573	1.83	(47)	20
74	SS, LS, chert	Nordegg	9-7-39-3W5	2182	5176	2896	1.79	(36)	10
75	SS, LS, chert	Nordegg	9-7-39-3W5	2183	4842	2726	1.78	(43)	15
76	SS, LS, chert	Nordegg	9-13-39-4W5	2193	4617	2664	1.73	(13)	17
77	SS, LS, chert	Nordegg	9-13-39-4W5	2194	5001	2864	1.75	(17)	12
78	SS, LS, chert	Nordegg	9-13-39-4W5	2195	4898	2847	1.72	(17)	15
79	SS, LS, chert	Nordegg	9-13-39-4W5	2196	5008	2960	1.69	(12)	12
80	SS, LS, chert	Nordegg	9-13-39-4W5	2197	5441	3157	1.72	(28)	13
81	SS, LS, chert	Nordegg	9-13-39-4W5	2198	5124	2937	1.74	(27)	12
82	SS, LS, chert	Nordegg	9-13-39-4W5	2199	4854	2924	1.66	(41)	9
83	LS, DL, SH	Shunda	9-5-39-3W5	2173	4570	2721	1.68	(85)	9
84	LS, DL, SH	Shunda	9-5-39-3W5	2174	4945	2721	1.82	(48)	8
85	LS, DL, SH	Shunda	9-5-39-3W5	2175	4771	2798	1.71	(69)	5
86	LS, DL, SH	Shunda	9-5-39-3W5	2176	5058	2821	1.79	(49)	5
87	LS, DL, SH	Shunda	9-5-39-3W5	2177	5366	2989	1.80	(41)	4
88	LS, DL, SH	Shunda	9-5-39-3W5	2178	5524	3096	1.78	(95)	3
89	DL, some SS	Detrital	9-13-39-4W5	2200	4451	2693	1.65	(64)	18
90	DL, some SS	Detrital	9-13-39-4W5	2201	4504	2684	1.68	(69)	18
91	DL, some SS	Detrital	9-13-39-4W5	2202	5089	2972	1.71	(74)	15
92	DL, some SS	Detrital	9-13-39-4W5	2203	6171	3375	1.83	(77)	5
93	DL, some SS	Detrital	9-13-39-4W5	2204	5763	3271	1.76	(80)	8
94	DL, some SS	Detrital	9-13-39-4W5	2205	5176	2674	1.94	(75)	11
95									
96	SS: Sandstone	LS: Limestone	SH: Shale	DL: Dolomite					

*Brackets suggest that this value indicates radioactivity but does not necessarily reflect shale content.